

# Volume backscattering of finite-amplitude acoustic waves: Power flow, sampled volume, and scattering cross section

Per Lunde<sup>a,b</sup>

University of Bergen, Dept. of Physics and Technology, P.O.Box 7803, N-5020 Bergen, Norway

Audun O. Pedersen<sup>c</sup>

Christian Michelsen Research AS, P.O.Box 6031, Postterminalen, N-5892 Bergen, Norway

## ABSTRACT

In multiple-target volume backscattering applications, the volume and cross-sectional area interrogated by the acoustic beam may be influenced by finite-amplitude sound propagation effects. To analyze the magnitude of such effects, generic governing equations for propagation and backscattering of small- and finite-amplitude signals in fluid media are formulated in terms of power budget equations, describing transmit-receive electrical power transfer functions, applicable to single-target and volume backscattering. Effective sampled area and sampled volume of the volume backscattering system are defined, accounting for two-way sound propagation and the transmit and receive properties of the transducer. Volume backscattering power flow is interpreted in terms of the equivalent backscattering cross section of the sampled volume. Expressions are given which describe how the sampled area, the sampled volume, and the backscattering cross-section of the sampled volume, are influenced by finite amplitude effects.

## I. INTRODUCTION

Acoustic backscattering is used in diverse applications, such as remote sensing, acoustic Doppler current profiling, fish abundance estimation, fish species identification, acoustic imaging, etc. Control with the volume and cross-sectional area being interrogated by the sound field, is important.

At long measurement ranges, or in noisy environment, challenges with low or marginal signal-to-noise ratio (SNR) may be experienced. In such situations, manufactures or users may be tempted to increase the electrical transmit power of the equipment. The resulting high sound pressure levels may introduce finite-amplitude effects as the sound signal propagates through the fluid medium. The chance of introducing finite-amplitude sound propagation effects increase with increasing frequency [1].

The volume and cross-sectional area interrogated by the acoustic beam (here referred to as the “sampled volume” and “sampled area”, respectively) are affected when finite-amplitude effects are present. The reason for that is the pressure dependency of the sound velocity in fluids [1]. The high and low pressure portions of the sound signal travel with different sound speeds, causing signal distortion. During propagation through the fluid medium, energy is transferred from the signal’s fundamental frequency component to the higher harmonic components. Consequently, for applications in which the fundamental frequency is the component exploited, the properties of the interrogating sound field are altered.

The sound pressure is highest at the main lobe. The fundamental frequency component’s loss of energy is thus

largest there, causing changed spatial distribution of the interrogating sound field, such as flattened beam pattern and increased beam width [1-4]. The altered beam pattern leads to changed sampled volume and area.

If not aware of or controlling such influences, a user may easily (and erroneously) assume that a different portion of the fluid volume is interrogated, than what is actually the situation. In applications of volume backscattering at high signal amplitudes, it is thus of interest to control and quantify how large the possible effects of finite amplitude are, such as with respect to changed sampled area and volume. The influence of range, frequency, and electrical transmit power is essential. Current literature appears to be sparse on expressions describing the effects of finite amplitude on the volume and cross-sectional area being interrogated by the sound beam in volume backscattering applications.

The objective of the present work is to improve on this lack of knowledge by giving expressions which describe how the sampled area, the sampled volume, and the backscattering cross-section of the sampled volume, are influenced by finite amplitude effects.

## II. ANALYSIS

A monostatic measurement situation with single-target and multiple-target (volume) backscattering is considered. Generic governing equations for propagation and backscattering of small- and finite-amplitude signals in fluid media are formulated in terms of power budget equations [5]. That is, in

<sup>a)</sup> Corresponding author. Electronic mail: per.lunde@ift.uib.no

<sup>b)</sup> Also with Christian Michelsen Research AS, P.O.Box 6031, Postterminalen, N-5892 Bergen, Norway; and the Michelsen Centre for Industrial Measurement Science and Technology, Norway.

<sup>c)</sup> Present address: ClampOn AS, Vaagsgaten 10, N-5160 Laksevaag, Bergen, Norway.

terms of transmit-receive electrical power transfer functions, applicable to single-target and volume backscattering. These equations apply under the assumption that certain stated approximations are valid [6,5]. These are assumptions underlying e.g. the conventional theory of fishery acoustics (abundance measurement, and species identification) [2,3,6]. For the finite-amplitude case, it is assumed that finite-amplitude effects are influent only for the forward-propagated signal, and not for the backscattered signal [5].

The small- and finite-amplitude power budget equations [6,5] are interpreted in terms of power flow, for single-target and for volume backscattering [7]. Effective sampled area and sampled volume of the volume backscattering system are defined, accounting for two-way sound propagation, and the transmit and receive properties of the transducer. These are denoted  $A_s$  and  $A_s^n$ , and  $V_s$  and  $V_s^n$ , respectively, for small-amplitude and finite-amplitude signals (with no superscript, and superscript “n”, respectively).  $A_s$  is defined as the cross-sectional area of the two-way equivalent beam solid angle, at range  $r$ .  $V_s$  is defined as  $A_s$  multiplied with one half of the transmitted signal length (in meters) [8]. Similar definitions are used for  $A_s^n$  and  $V_s^n$  [7]. Expressions are derived for the sampled area and sampled volume [7].

Volume backscattering power flow is interpreted in terms of the equivalent backscattering cross section of the sampled volume [8,7]. These are denoted  $\sigma_{bs}^v$  and  $\sigma_{bs}^{v,n}$ , for small-amplitude and finite-amplitude signals, respectively. For the precise definitions and analysis of these quantities, it is referred to Appendix B of [8], and [7].

For finite-amplitude signals, the expressions for the sampled area, sampled volume, and the equivalent backscattering cross section of the sampled volume, are compared with the corresponding expressions for small-amplitude signals. It is found that [7]

$$\frac{A_s^n}{A_s} = \frac{V_s^n}{V_s} = \frac{\sigma_{bs}^{v,n}}{\sigma_{bs}^v} = \psi_{rel}^n(r), \quad (1)$$

where a “beam angle finite-amplitude factor” is introduced, defined as

$$\psi_{rel}^n(r) \equiv \frac{\psi^n(r)}{\psi} = \frac{\int_{4\pi} |\mathbf{B}_i(\theta, \varphi)|^2 \cdot |\mathbf{B}_i^n(r, \theta, \varphi)|^2 d\Omega}{\int_{4\pi} |\mathbf{B}_i(\theta, \varphi)|^4 d\Omega}. \quad (2)$$

Here,  $\psi$  [2,3,6,9,10] and  $\psi^n(r)$  [4,5] are the equivalent two-way beam solid angles of the transducer, for small- and finite-amplitude signals, respectively.  $\mathbf{B}_i(\theta, \varphi)$  and  $\mathbf{B}_i^n(r, \theta, \varphi)$  are the beam patterns of the incident sound pressure wave, at small- and finite-amplitude conditions, respectively. That is, the angular distributions of the sound pressure, respectively, normalized to the respective axial sound pressures at the same range [5].

For finite amplitude signals, one has  $\psi_{rel}^n(r) > 1$ , so that  $A_s^n > A_s$ ,  $V_s^n > V_s$ , and  $\sigma_{bs}^{v,n} > \sigma_{bs}^v$ . For given range and frequency, the sampled area, sampled volume, and the equivalent backscattering cross section of the sampled volume, thus increase with increasing signal amplitude, until full saturation occurs, and constant values are reached.

At large ranges,  $\mathbf{B}_i^n(r, \theta, \varphi)$ , and thus  $\psi_{rel}^n(r)$ , and therefore also  $A_s^n/A_s$ ,  $V_s^n/V_s$ , and  $\sigma_{bs}^{v,n}/\sigma_{bs}^v$ , become approximately constant, for a given frequency and a given source level.

For a given transducer, frequency, and electrical transmit power level,  $\mathbf{B}_i(\theta, \varphi)$  and  $\mathbf{B}_i^n(r, \theta, \varphi)$ , and thus  $\psi$ ,  $\psi^n(r)$ , and  $\psi_{rel}^n(r)$ , can be measured. [In fisheries acoustics, for example,  $\psi$  is provided on a routinely basis by many echosounder manufacturers [10].] Alternatively, these quantities can be calculated using numerical models, such as e.g. the “Bergen Code” [11] based on the KZK equation [12,13], or similar models [1].

### III. EXAMPLE RESULTS

To illustrate typical magnitudes of effects which may be expected, an example is taken from fisheries acoustics (abundance estimation). Two scientific echo sounders are considered, Simrad ES120-7C and ES200-7C, operating at 120 and 200 kHz, respectively [4]. The half-power (-3dB) angles of both transducers are 3.5° (nominal values), with measured values of  $10\log(\psi/1\text{sr})$  equal to -21 and -20.5 dB re. 1 sr, for the 120 and 200 kHz transducers, respectively [4].

The “Bergen Code” is used for calculations of the radiated sound fields of these transducers for small- and finite-amplitude signals, over the ranges 12-300 m. As a simplified (but still relevant) approach, the transducers are assumed to vibrate as uniformly vibrating circular planar pistons, mounted in a rigid baffle of infinite extent. The effective piston radii of the two transducers are taken to be 52.8 and 32.0 mm, respectively, obtained from tank measurements of the transducers’ far field beam patterns at small-amplitude conditions [4]. For small-amplitude signals, the source condition pressure amplitude  $P_0$  is taken to be 1 Pa. For finite-amplitude signals,  $P_0$  is scaled by the voltage amplitude measured across the transducer’s electrical terminals upon signal transmission. For the 120 kHz transducer,  $P_0$  values of  $1.90 \cdot 10^5$  and  $3.96 \cdot 10^5$  Pa were used, for electrical transmit powers of 250 and 1000 W, respectively. For the 200 kHz transducer,  $P_0$  values of  $2.63 \cdot 10^5$  and  $7.92 \cdot 10^5$  Pa were used, for electrical transmit powers of 120 and 1000 W, respectively [4]. The density and sound speed of seawater are taken to be 1027 kg/m<sup>3</sup> and 1491 m/s, respectively, and the nonlinearity coefficient is set to  $\beta = 3.59$ . The absorption coefficient of seawater  $\alpha$  is - somewhat simplified with respect to its frequency dependency - taken to be  $3.06 \cdot 10^{-13} \cdot f^2$  and  $1.57 \cdot 10^{-13} \cdot f^2$  Np/m, for the 120 and 200 kHz signals, respectively.

Fig. 1 shows  $\psi_{rel}^n(r)$  calculated as a function of range,  $r$ , for the 120 and 200 kHz echo sounders. Two power settings are used for each echo sounder frequency (corresponding to “low” and “high” electrical transmit power levels): 120 kHz at 250 and 1000 W, and 200 kHz at 120 and 1000 W. From Eq. (1), it follows that Fig. 1 also describes the change of  $A_s^n/A_s$ ,  $V_s^n/V_s$ , and  $\sigma_{bs}^{v,n}/\sigma_{bs}^v$ , as a function of range,  $r$ , for the frequencies and power settings given above.

An example may be illustrative. Consider the case  $r = 100$  m,  $f = 200$  kHz, electrical transmit power = 1000 W, and pulse duration = 1 ms (corresponding to a pulse length of about 1.5 m in seawater). From Fig. 1 it follows that  $\psi_{rel}^n(r) \approx 1.29$ . From expressions given in [7], it can be shown that for small-amplitude signals, the sampled area and sampled volume become  $A_s \approx 78.5$  m<sup>2</sup> and  $V_s \approx 58.9$  m<sup>3</sup>, respectively. For finite-amplitude signals (“high” power setting, 1000 W), the sampled area and sampled volume increase by a factor 1.29 to  $A_s^n \approx 101.3$  m<sup>2</sup> and  $V_s^n \approx 76.0$  m<sup>3</sup>, respectively. For the radius of the sampled area, this corresponds to an increase from 5.0 m to about 5.7 m, due to the increased electrical transmit power.

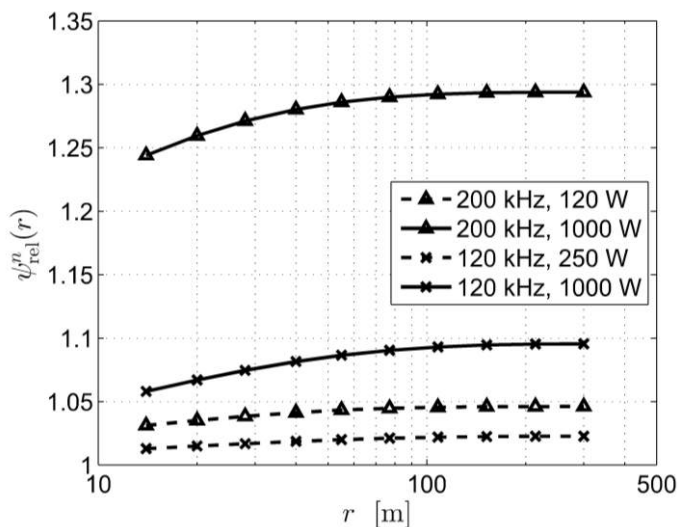


Fig. 1. Beam angle finite-amplitude factor,  $\psi_{rel}^n(r)$ , simulated using the KZK equation as a function of range,  $r$ , for two echo sounder frequencies, 120 and 200 kHz, at two different electrical transmit power levels for each frequency.

#### IV. CONCLUSIONS

It has been shown that for finite-amplitude signals in multiple-target (volume) backscattering applications, the sampled volume, the sampled area, and the backscattering cross section of the sampled volume, at given range and frequency, all increase proportional to  $\psi_{rel}^n(r)$ . That is, proportional to the quotient of the equivalent two-way beam solid angles at finite- and small-amplitude conditions, respectively. The expression for  $\psi_{rel}^n(r)$  is given in terms of the transducer’s beam patterns at finite- and small-amplitude conditions, which can

relatively easily be measured at laboratory conditions, or calculated. Example calculations are given here.

The analysis is relatively generic, and derived under a set of well defined assumptions (conditions). The results are expected to apply to a relatively wide range of acoustic backscattering systems operating in fluid media.

#### ACKNOWLEDGMENTS

Part of the work has been supported by the Research Council of Norway (MARE 152790), and Fiskeri- og havbruksnæringens forskningsfond, Norway (FHF 222042).

#### REFERENCES

- [1] *Nonlinear Acoustics*, edited by M. F. Hamilton and D. T. Blackstock (Academic Press, San Diego, CA, 1998), 455 p.
- [2] C. S. Clay and H. Medwin, *Acoustical oceanography: Principles and applications* (J. Wiley & Sons, New York, 1977), pp. 180-182, 205, 220, 225-235, and 395-404.
- [3] H. Medwin and C. S. Clay, *Fundamentals of acoustical oceanography* (Academic Press, Boston, 1998), pp. 153-158, 350-361.
- [4] A. Pedersen, *Effects of nonlinear sound propagation in fisheries research* (Ph.D. thesis, University of Bergen, Dept. of Physics and Technology, Bergen, Norway, 2006), 307 p. URL: [https://bora.uib.no/handle/1956/2158?mode=full&submit\\_simple=Show+full+item+record](https://bora.uib.no/handle/1956/2158?mode=full&submit_simple=Show+full+item+record). (Accessed March 16, 2015.)
- [5] P. Lunde, "Finite-amplitude power-budget equations for acoustic fish abundance estimation", Unpublished manuscript, Dept. of Physics and Technology, University of Bergen, Norway (2015). To be published.
- [6] P. Lunde, A. O. Pedersen, R. J. Korneliussen, F. E. Tichy, and H. Nes, "Power-budget and echo-integrator equations for fish abundance estimation", *Fisken og Havet* no. 10/2013, Institute of Marine Research, Bergen, Norway (2013), 39 p. URL: [http://www.imr.no/publikasjoner/andre\\_publicasjoner/fisken\\_og\\_havet/nb-no](http://www.imr.no/publikasjoner/andre_publicasjoner/fisken_og_havet/nb-no). (Accessed March 16, 2015.)
- [7] P. Lunde and A. O. Pedersen, "Acoustic sampling volume in backscattering of finite-amplitude incident sound", Unpublished manuscript, Dept. of Physics and Technology, University of Bergen, Norway (2015). To be published.
- [8] P. Lunde and R. J. Korneliussen, "A unifying theory explaining different power budget formulations used in modern scientific echosounders for fish abundance estimation", *Fisken og Havet* no. 7/2014, Institute of Marine Research, Bergen, Norway (2014), 32 p. URL: [http://www.imr.no/publikasjoner/andre\\_publicasjoner/fisken\\_og\\_havet/nb-no](http://www.imr.no/publikasjoner/andre_publicasjoner/fisken_og_havet/nb-no). (Accessed March 16, 2014.)
- [9] C. A. Balanis, *Antenna theory: Analysis and design*, 3<sup>rd</sup> ed. (J. Wiley & Sons, Hoboken, New Jersey, 2005), pp. 50, 66, 89-95.
- [10] "Operator manual: SIMRAD EK500 Fishery research echo sunder. Scientific echo sunder: Base version", Doc. no. P2170 / Revision G, Simrad AS (now Kongsberg Maritime AS), Horten, Norway (1997), "Section 7: Theory of operation", pp. 165-169, and Appendix "Calibration of the EK500", p. 211-212. URL: <http://www.simrad.com/www/01/nokbg0397.nsf/AllWeb/93FDCCAD1CC54473C12573F50076A3C4?OpenDocument> (Accessed March 16, 2015.)
- [11] J. Berntsen, J. Naze Tjøtta, and S. Tjøtta, "Interaction of sound waves. Part IV: Scattering of sound by sound", *J. Acoust. Soc. Am.* **86**(5), 1968-1983 (1989).
- [12] E. A. Zabolotskaya and R. V. Khokhlov, "Quasi-plane waves in the nonlinear acoustics of confined beams", *Sov. Phys. Acoust.* **15**(1), 35-40 (1969).
- [13] V. P. Kuznetsov, "Equations of nonlinear acoustics", *Sov. Phys. Acoust.*, **16**(4), 467-470 (1971).